

27
4/16/79
2490
UTIS
SAND78-2287
Unlimited Release

GAS PERMEABILITY OF SENM ROCK SALT

H. J. Sutherland

S. Cave



Sandia Laboratories

SF 2900 G(7-73)

MASTER

DISSEMINATION OF THIS DOCUMENT IS UNLIMITED

GAS PERMEABILITY OF SEMI ROCK SALT*

by

Herbert J. Sutherland
Sandia Laboratories†
Albuquerque, New Mexico 87185

and

Steven P. Cave
Missouri Research Laboratories, Inc.
Albuquerque, New Mexico 87102

*This work was supported by the U. S. Department of Energy.

†A DOE facility.

NOTICE

This report was prepared as an account of work sponsored by the United States Government. Neither the United States nor the United States Department of Energy, nor any of their employees, nor any of their contractors, subcontractors, or their employees, makes any warranty, express or implied, or assumes any legal liability or responsibility for the accuracy, completeness or usefulness of any information, apparatus, product or process disclosed, or represents that its use would not infringe privately owned rights.

ABSTRACT

Laboratory measurements of the argon gas permeability for rock salt specimens from the Waste Isolation Pilot Plant (WIPP) site in Southeast New Mexico (SENM) are obtained by using a transient, pressure-step technique. Hydrostatic and differential pressure states are investigated as a function of confining pressure and time. These data, when combined with the results of other experimenters, lead to the conclusions that the in-situ permeability of the undisturbed formation is less than $0.05 \mu\text{d}$; the introduction of non-lithostatic stress states into the formation, as with mining, may produce connected porosity that will increase the permeability of the formation; and, hydrostatic pressure states applied for finite time periods tend to "heal" the formation to its original undisturbed state.

TABLE OF CONTENTS

INTRODUCTION	1
EXPERIMENTAL PROCEDURES	2
Permeability Measurement System	2
Specimen Preparation	4
Testing Procedure	5
RESULTS	6
Calibration	6
Hydrostatic Test Results	7
Differential Stress Test Results	9
OTHER MEASUREMENTS	11
Core Labs	12
Terra Tek	12
Shelby	13
DISCUSSION	13
CONCLUSION	16
REFERENCES	17
TABLES	18
I Hydrostatic Pressure, Summary of Results, Spec. No. 9-2103	18
II Hydrostatic Pressure, Summary of Results, Spec. No. 9-2105	19
III Hydrostatic Pressure, Summary of Results, Spec. No. 9-2601.5	21
IV Hydrostatic Pressure, Summary of Results, Spec. No. 9-2609	22

V	Hydrostatic Pressure, Summary of Results, Spec. No. 9-2610	23
VI	Hydrostatic Pressure, Summary of Results, Spec. No. 9-2613	24
VII	Hydrostatic Pressure, Summary of Results, Spec. No. 9-2671.5	25
VIII	Differential Pressure, Summary of Results, Spec. No. 9-2610	26
IX	Differential Pressure, Summary of Results, Spec. No. 9-2613	27
FIGURES		28
1	Test Data from Test 11B-1, 9-2613	28
2	Logarithmic Data from Test 11B-1, 9-2613	29
3	Experimental Setup	30
4	Test Series A for 9-2103	31
5	Test Series A for 9-2609	32
6	Test Series B for 9-2105	33
7	Test Series B for 9-2613	34
DISTRIBUTION		35

INTRODUCTION

Historically, "containerless" storage of liquids and gases in cavities mined into stable geological formations of rock salt has been studied and used as a method for safely storing large volumes of hydrocarbons for long periods of time (e.g., see Ref. 1, 2, and 3). More recently, studies have indicated that these same formations could also be used to safely store solid nuclear wastes. One formation under study for this purpose is located in Southeast New Mexico (SENM) and is called the Waste Isolation Pilot Plant (WIPP). A proposal for this pilot plant is to store low level transuranic (TRU) wastes. These wastes are in combination with organic materials which, if not placed in the repository in an incinerated condition, will be broken down into gases by bacterial decomposition, pyrolysis, and radiolysis. As the quantity of gas produced is expected to be quite large over geological time scales, the permeability of the surrounding formation becomes an important parameter for determining the manner in which the gases will be contained or dispersed.

This paper reports the results of gas permeability studies, conducted by the authors, on specimens from this site in SENM that were obtained by core drilling the rock salt formation. The permeability studies of Core Labs⁴ and Terra Tek⁵ on this same formation and the studies of Shelby⁶ on single crystal sodium chloride are also discussed. Conclusions are then drawn about the in-situ permeability of the formation and the effect of differential stress states on this permeability.

EXPERIMENTAL PROCEDURES

The gas permeability measurements reported here are for core samples taken from hole EFDA-9 at the WIPP site in GENM. All tests were conducted using the transient method,⁷ and were conducted according to the procedures established by the American Petroleum Institute (API)⁸. Each test measured the permeability of a sample to argon gas, along its axis (the bore hole axis), as it was being subjected to a hydrostatic pressure state or a differential pressure state.

Permeability Measurement System

The apparatus used to measure the gas permeability of the rock salt samples uses the transient method,⁷ in which an incremental pressure difference ΔP_0 between a large gas volume V_1 and a small gas volume V_s are allowed to equilibrate through a sample of length l and cross sectional area A . As shown in Ref. 7, if Darcy's Law is valid and $V_1 \gg V_s$, then the pressure difference across the sample ΔP at time t is given by:

$$\Delta P = (\Delta P_0) e^{-\alpha t} \quad , \quad (1)$$

where

$$\alpha = K \left(\frac{A}{l} \right) \left(\frac{1}{V_s} \right) \left(\frac{1}{\mu \beta} \right) \quad . \quad (2)$$

Here, μ and β are the viscosity and bulk modulus, respectively, of the gas and K is the permeability of the specimen. Solving (1) and (2) for the permeability yields

$$K = S \left(\frac{l}{A} \right) V_s \mu \beta \quad , \quad (3)$$

where

$$s = \frac{d}{dt} \left[\ln \left(\frac{\Delta P}{P_0} \right) \right] . \quad (4)$$

For the system used, the large volume was approximately $2.3 \times 10^{-3} \text{ m}^3$ (140 in^3) and the small volume was approximately $1.3 \times 10^{-5} \text{ m}^3$ (0.8 in^3).^{*} The maximum working pressure of the argon, i.e., its absolute pressure, was 10.3 MPa (1500 psi) and the maximum initial differential pressure was 0.69 MPa (100 psi). The working pressure of the system was measured using an electrical absolute pressure gauge, and the pressure across the sample was measured using a diaphragm-type electrical differential pressure gauge. All data was recorded using a minicomputer and a strip chart recorder.

Typical data, from Test 11B-1 on specimen 9-2613^{**} are shown in Fig. 1. For this test, the initial differential pressure P_0 was approximately 0.31 MPa (45 psi), and the test was started between the fourth and fifth data points. This exponentially decaying pressure curve is plotted in logarithmic form in Fig. 2. A least squares curve fit was used to determine the slope S , Eq. (4), for inclusion into Eq. (3). The viscosity and bulk modulus for the argon was determined from the data present in Ref. 9. The dimensions of the specimen were determined before the test and were not corrected for strain states imposed on the specimen during the course of the measurements.

At this point, it seems warranted to point out the conditions necessary for Darcy's Law to be valid; i.e., the conditions which permit the derivation of Eq. (1). These conditions include: (1) viscous, one-dimensional flow with a linear pressure drop along the length of the sample;

^{*} The large volume was determined by calculating the size of each piece of the apparatus and the small volume was determined dilatometrically. (This technique will be discussed later.)

^{**} The notation used to specify samples is bore hole-horizon depth; i.e., this specimen came from bore hole number 9 and its depth was 2613 feet.

(2) no "capacity" change in the specimen during testing; i.e., the connected porosity of the specimen remains constant; (3) no chemical reactions; (4) no electro-kinetic effects; and (5) no "slip" at the gas/flow channel interface. An additional condition for the tests reported here is that (6) there is only argon gas in the specimen and permeability apparatus. Implications of these conditions on the measured results will be discussed later in the paper.

Specimen Preparation

The specimens tested here were obtained from bore-hole ERDA 9 at depths of approximately 640 m (2100 ft) and 792 m (2600 ft). The raw core had a diameter of 108 mm (4.25 in) and came in various lengths. These lengths were cut and their ends were ground flat to obtain cylindrical specimens of "raw" core that were approximately 102 mm (4 in) long. The lateral surfaces of these cylinders were ground, to remove surface blemishes, to obtain "machined" core that had a diameter of approximately 76 mm (3.9 in). Special care was taken in machining to avoid damaging the fabric of the core samples.

The technique used to prepare a specimen for testing is shown in a cut-away view in Fig. 3. The procedure was to first fill any surface blemishes on the lateral surfaces of the specimen with RTV silicone rubber and then to paint three layers of the RTV, thinned with toluene, onto this surface. Each layer was allowed to dry (cure) before the next layer was applied. The specimen was then attached to the stainless steel (SST) end caps shown in Fig. 3. A layer of porous SST felt was placed between the caps and the specimen to insure that the gas introduced through the end caps to the specimen was able to cover the entire end surfaces of the specimen. The lateral surface of the end cap was sealed to that of the

specimen using a band of Viton rubber that was approximately 2.5 mm (0.1 in) thick and 51 mm (2 in) wide. This band was placed over the gap between the two (with the felt between them) and then RTV was forced between the band and the lateral surfaces.* The assembly was then covered with a polyurethane or Viton jacket, which was sealed on its ends with RTV and safety wires.

Testing Procedure

The specimens were tested at an ambient temperature of $22.8^{\circ} \pm 1^{\circ} \text{C}$ ($73^{\circ} \pm 2^{\circ} \text{F}$) in the creep apparatus developed by Wawersik.¹⁰ Two stress states were investigated: (1) hydrostatic pressure and (2) differential stress at constant confining pressure. For both types, the specimen assembly, Fig. 3, was loaded into the testing frame and a hydrostatic pressure was applied.** To remove gases trapped in the specimen, the specimen was then placed under a vacuum (via the gas ports in the end caps, see Fig. 3), purged with argon, reevacuated, and filled with argon. The permeability apparatus and the sample were allowed to come to equilibrium, and then the first measurements were made. This process took from 0.5 to 2 hrs, depending on the initial permeability of the specimen. All times were measured from the application of the hydrostatic pressure.

For the hydrostatic pressure tests, permeability measurements were made after the specimen/apparatus system had been allowed to return to a state of (quasi) equilibrium after a pressure change. This condition was assumed when the pressure in the large volume side of the apparatus and the pressure in the small volume/specimen side of the apparatus remained

* Some RTV was forced onto and into the felt, but post-test examination revealed that this penetration (and subsequent blocking of the felt) was always less than 2.5 mm (0.1 in) around the circumference.

** The gas pressure in the permeability apparatus was always kept less than this hydrostatic pressure.

constant for approximately 5 min. For differential stress states, the strain rate was kept constant at approximately 0.21 MPa/min (31 psi/min), thus following the stress paths reported by Wawersik and Hannum.¹¹ The permeability measurement was always taken near the end of a differential pressure step. The implications of this procedure for differential stress state measurements will be discussed later.

RESULTS

The results for the seven specimens tested here are reported in Tables I to IX, and selected results are shown graphically in Fig. 4 to 7. Three general classes of tests were conducted on these specimens. Type A tests were confining pressure/time tests (zero differential stress) on raw core samples (see Tables I to VII). Type B tests were also confining pressure/time tests but were conducted on machined and, sometimes, pretested samples (see Tables I to VII). Type C tests were the constant confining pressure tests in which the differential stress was raised as a function of time (see Tables VIII and IX).*

Calibration

To test the specimen sealing technique and to calibrate the system, a solid aluminum sample was prepared exactly like a salt sample and was tested. The first series of tests demonstrated that the sealing technique prevented gas from flowing around the sample when the confining pressure was at least 0.35 MPa (50 psi) greater than the gas pressure.

*The principle stress along the axis of the sample was increased.

The jacketed aluminum sample also allowed the small volume to be measured accurately using a dilatometric technique. In this technique, the small volume was changed a small, known amount by using a sealed piston that was incorporated into the small volume for this purpose. The resulting pressure change was measured and the small volume was calculated using the known bulk modulus of argon gas.

Based on these tests, and subsequent tests of salt samples, the minimum permeability that could be measured for the sample sizes used here was determined to be $0.05 \mu\text{d}$.^{*} The experimental error was estimated to be $\pm 4\%$ or $\pm 0.03 \mu\text{d}$, whichever is greater.

Hydrostatic Test Results

The results for the seven specimens tested under hydrostatic pressure are tabulated in Tables I to VII. Selected results are shown graphically in Fig. 4 to 7. Series A tests on specimens 9-2103, 9-2609, and 9-2613, see Tables I, IV, and VI, were conducted first, and were used, more or less, as a series of scoping tests to determine pertinent parameters to be studied and to evaluate, as much as possible, the assumption that Darcy's Law was valid for these tests.

For the latter, one assumption that leads to the validation of Darcy's Law, that can be checked experimentally, is the condition of no slip. As discussed in Ref. 8, 12, and 13, the permeability of a specimen to a gas is a function of the absolute pressure of the gas (we called this the working gas pressure). In particular, as the absolute pressure of the gas increases, the apparent permeability of the specimen decreases

* Assuming that Darcy's Law is valid for this low flow regime.

asymptotically to the so-called "liquid" permeability for a gas.* This asymptote corresponds to the condition of no slip. As seen in tests 15A, 16A, and 17A for specimen 9-2609 (Table IV), the gas pressure was reduced from 10.4 MPa (1515 psi) to 7.0 MPa (1010 psi), and then to 3.48 MPa (505 psi). For all of these tests the confining pressure was held approximately constant at 14.0 MPa (2030 psi)** and all tests were conducted within an hour of each other. The results illustrated that the permeability is constant, within experimental accuracy, for these tests. Thus, the permeability measurements reported here are for the condition of no slip, and the values measured are the so-called "liquid" permeability for these samples.

During the course of a test series, the gas flow through the specimen is normally from the large volume to the small volume for our permeability apparatus. To determine if flow channels had been "plugged" by material transport in one direction, several tests were conducted in which the flow was reversed, see Tables I, V, and VI. As seen in these tables, the measurements are essentially unchanged.

Also, during the initial series of tests, many measurements were repeated. As seen in Tables I, IV, and VI and Figs. 4 and 5, repeated measurements were almost always less than their original value. This observation implies that time at pressure was influencing the measurements. A long-term test on specimens 9-2105 confirmed this hypothesis, and the results, shown in Fig. 6 display the importance of this parameter.

* Klinkenberg¹³ showed that the permeability is approximately a linear function of the reciprocal mean pressure, and that this effect can be explained by taking into account the phenomena of slip, which is related closely to the mean free path of the gas molecules. This phenomenon is commonly called "Klinkenberg slip".

** For test 1A and 1B in this same table, an interval of approximately 2 hrs. passed between the two tests. This long period of time at the beginning of the stress cycle invalidates these two tests for this comparison (time effects will be discussed later).

After these initial test series, additional tests were conducted on other specimens and then the specimens were machined and some were re-tested. The results from these tests are also tabulated in Tables I to VII.

Specimens 9-2601.5 and 9-2671.5 (Tables III and VII respectively) are somewhat different than the other specimens tested. These specimens were pretested by *Wawersik*¹¹ to determine their mechanical properties. Specimen 9-2601.5 had been tested at room temperature and constant confining pressure of 20.7 MPa (3000 psi) to a principle stress difference of 60 MPa (8700 psi). The permeability test on this sample was conducted approximately 6 months after its initial test. Specimen 9-2671.5 had also been tested at room temperature. It was tested at approximately constant principle stress difference and then constant confining pressure of 1.7 MPa (250 psi) to 34.5 MPa (5000 psi) differential stress.

Differential Stress Test Results

The results of the constant confining pressure, differential stress measurements are tabulated in Tables VIII and IX. As discussed earlier, the stress rate for both tests was 0.21 MPa/min (31 psi/min). For tests on specimen 9-2610, this stress rate was achieved by 6.9 MPa (1000 psi) steps every 32 min., and for specimen 9-2613, by 3.5 MPa (500 psi) steps every 16 min.* Both specimens were "healed"^{**} before testing. The stress cycle for specimen 9-2610 was a constant confining pressure of 13.8 MPa (2000 psi) with a rise to 55.2 MPa (8000 psi) differential stress and then dropping the different stress back to zero. Total test time was approximately 4.5 hrs. The stress cycle for 9-2613 was much more complicated. With a constant confining pressure of 20.7 MPa (3000 psi), the different stress was

* Engineering stress is quoted for all the differential stress measurements.

** This term will be discussed later.

raised to 41.4 MPa (6000 psi); lowered to zero and left over night; and then raised to 69.0 MPa (10,000 psi) the next day. Total test time was approximately 27 hrs.

After the tests were completed, the specimens were checked for total volumetric and axial strain. For specimen 9-2610, the volumetric strain was +4.5% and the axial was 13.9%. For 9-2613, they were -0.5% and +21.6% respectively. It should be pointed out at this point that these values will be different from those obtained by Wawersik.^{10,11} This difference is a result of different end constraints on the specimens being tested. For Wawersik's tests, the mating surfaces were smooth and greased, but for these tests, the stainless steel felt (used to vent the ends of the specimen) was comparatively rough and had a distinct tendency to restrain the ends of the specimen; thus, causing the disparities between the two sets of data.

For both of these tests, a problem developed with the measurement scheme when the differential stress exceeded approximately 27.6 MPa (4000 psi). In particular, when the specimen was connected to the small volume, the pressure in the small volume began to change implying that the capacity of the rock was changing. This change made one assumption for the derivation of Eqs. (1) to (4) invalid, but since the rate of the capacity change was approximately constant at the end of both the 16 and 32 time steps, an apparent permeability was computed by correcting the pressure decay ΔP (see Eq. 1) for the pressure change resulting from this capacity change and then computing the slope S (Eq. 4) to determine the "apparent" permeability. Obviously, these numbers are in error and are quoted here only to establish trends for stress rates comparable with the

work of other experimenters.^{10,11} Future tests must be run under stress rate conditions which allow the capacity change to come to some (quasi-) equilibrium.

For these two tests, the capacity increased in specimen 9-2610 and decreased in specimen 9-2613.* In particular, at approximately 13.8 MPa (2000 psi) confining pressure, the capacity of specimen 9-2610 started to increase at the 34.5 MPa (5000 psi) level and continued to increase until the differential pressure was lowered to zero (see Table VIII). At 20.7 MPa (3000 psi) confining pressure, the capacity specimen 9-2613 started to decrease and continued to decrease up to the 41.4 MPa (6000 psi) level. After lowering the differential pressure to zero, holding the specimen overnight at the 20.7 MPa (3000 psi) confining pressure, and then reapplying the differential stress, the capacity started to decrease again at the 41.4 MPa (6000 psi) level. The capacity continued to decrease for the remainder of the differential stress states.

OTHER MEASUREMENTS

Two other experimenters have investigated the permeability of SENM rock salt from the WIPP site and one other has investigated the permeability of single crystal sodium chloride. As these data bear directly on the conclusion drawn later in this paper, a brief summary of their work is provided.

*The capacity of the rock is decreasing if the pressure in the small volume is increasing, and vice versa.

Core Labs

Core Labs performed many permeability measurements on core from ERDA 9.⁴ The description of their technique is sketchy, but they report that they did follow the API recommended procedures.⁸ Their technique, probably, was to use full core specimens that had been machined on their ends and "dried" (?). Air (nitrogen?) permeability was then determined at atmospheric pressure (?). As this gas pressure is comparatively low, their data will probably be higher than the "liquid" permeability for a gas.

The measured air permeability ranged from 0.17 md to 0.4 μ d for specimens from approximately 622 m (2040 ft) and from 16 md to 0.4 μ d for specimens from approximately 814 m (2670 ft).

Terra Tek

Terra Tek is performing gas permeability measurements on full size core samples from ERDA 9 at an approximate depth of 829 m (2750 ft).⁵ This work is being conducted under contract to Sandia. Their technique and apparatus is essentially the same as the one used by Sandia (designed independently). Measurements were made for nitrogen and hydrogen gas with confining pressures to 29.0 MPa (4200 psi). The gas pressure is approximately 0.22 MPa (32 psi); thus, their data are also probably high when compared with the "liquid" permeabilities for a gas.

The permeability measured for both nitrogen and hydrogen follow the trends reported for argon; namely, the measured permeability is erratic at first, but decreases steadily with the application of confining pressure and with increased time at pressure. After some pressure/time history was imposed, the hydrogen permeability was reduced to less than 0.05 μ d, and for nitrogen, less than 0.1 μ d (the reduction of their apparatus).

Shelby

Shelby, of Sandia Labs Livermore, conducted gas permeability measurements on single crystal sodium chloride. His technique requires measurements at higher temperatures than of interest here, but when extrapolated to 40°C, the measured permeability for deuterium was less than 10^3 molecules/s-cm-atm. This value corresponds to a diffusion coefficient of 2×10^{-9} cm²/sec. To place these numbers in engineering terms, one can assume argon gas at 10.3 MPa (1500 psi) and at room temperature, and calculate that the permeability is less than one pd. This value of one pd is representative of the other gases under study.

DISCUSSION

As with most laboratory investigations of geological materials, the objective of this work was to use controlled experiments in a laboratory environment to estimate the in-situ properties of the specimens under study. As the rock salt formation in SENM has been stable over geological time scales and the salt has the ability to flow,^{10,11} the undisturbed formation is probably in a state of simple hydrostatic compression. Thus, the hydrostatic tests are probably the best indication of the undisturbed permeability of this formation. Using this rationale, four conclusions may be drawn from the existing data:

(1) The Core Labs data, and the short time/low confining pressure data reported here and by Terra Tek illustrate that the measured permeability of as-received core varies by three to five orders of magnitude, even when the specimens were very close to each other in the formation. As the material variability is not that great between specimens and the ability of salt to flow implies that the in-situ stress state of specimens from similar depths

¹¹This procedure is questionable because at these very low permeabilities, Darcy's Law is probably invalid.

will be essentially the same, one rapidly draws the conclusion that the permeability measurements on as-received core do not correlate to each other; i.e., the measured permeability is essentially meaningless for inferring the in-situ permeability of the formation.

A possible correlation of these data is based on the observation that the specimens are extremely friable, and any bump or jolt will tend to open the sample and increase its permeability. Thus, the sample exhibiting the lowest permeability has had the least damage, and its permeability is probably most representative of the in-situ permeability. These values are of the order of 0.3 μd , and may go down to less than 0.05 μd . But as seen in the tables presented here, even very careful machining increases the permeability of the specimens. Thus, even these numbers are suspect because of the coring process itself.

(2) The data obtained by Terra Tek and Sandia illustrate that the specimens behave as if they are "healing"* when subjected to confining pressures for some period of time. The effect is seen graphically in Figs. 6 and 7. These figures show that for both raw and machine core, when the in-situ hydrostatic pressure state is approximated by the application of a 13.8 MPa (2000 psi) confining pressure, the measured permeability holds constant for a relatively short "incubation" period and then begins to decrease. As seen in Fig. 7 the rate of decrease is a function of the pore pressure (and several other variables), but even after 200 hrs at pressure, the measured permeability is still decreasing. And, subsequent increases in the confining pressure reduced the measured permeability

*The term "healing" is used here to mean a return to the in-situ state. The governing mechanism, whether it be a true healing process or a consolidation process or something else is only a subject for speculation at this time.

even further (see Tables II and VI). Figs. 4 and 5 illustrate that similar results were achieved over shorter periods of time by increasing the confining pressure. For example, specimen 9-2103 was "healed" in 6 hrs to the same degree as specimen 9-2105 was healed in approximately 200 hrs by increasing the confining pressure from 13.8 MPa (2000 psi) to 34.5 MPa (5000 psi).

This healing process appears, for the most part, irreversible, in that once an imposed pressure/time history has reduced the measured permeability, subsequent reductions in the confining pressure produce only minor increases in the permeability and even overnight exposure to no confining pressure produces little increase (e.g., see Table I).*

(3) Based on the damage discussions in (1) and (2), one should choose the smallest measured permeability for a given horizon as the best laboratory duplication of the in-situ permeability. As the salt deposit has been essentially undisturbed for an extremely large period of time, the value chosen should probably be after the laboratory specimen has been artificially "healed" by a pressure/time history. Thus, the best duplication in the laboratory of the in-situ permeability is the same for argon, nitrogen, and hydrogen, and has a value of less than 0.05 μ d. This value may be even less because it is the resolution of the apparatus that was used to measure permeability of the specimens.

(4) The work of Shelby has shown that NaCl crystals are essentially impervious to gases. As his value of permeability is four orders of magnitude less than the measured permeability for core samples, the movement of the gas through the core samples is probably around the crystals and not through them.

* Terra Tek is investigating the possibility that this healing process is reversible over long periods of time.

Starting with the premise that the effects of coring, handling, and machining on a particular specimen can be eliminated in the laboratory by first healing the specimen with a pressure/time history, the effects of stress states that might be introduced into the formation by mining operations can be investigated. The primary investigations here were for constant confining pressure with increasing differential stress. For relatively high confining pressures of 13.8 MPa (2000 psi) or greater, some increase with differential stress is observed. This may (see Table VIII and IX) or may not (see Table III) be reversible.* For relatively low confining pressures of 3.5 MPa (500 psi), the increase in permeability can become very dramatic (see Table VII). Thus, the dilatant behavior observed in SENM rock salt,^{10,11} produces interconnected porosity (i.e., a capacity change) in the rock salt that increases its permeability.

CONCLUSION

Laboratory measurements of gas permeability for rock salt specimens from the WIPP site in SENM have led to the conclusion that the in-situ permeability of the undisturbed formation is less than 0.05 md. And, the introduction of non-lithostatic stress states into the formation, as with mining, may produce connected porosity that will increase the permeability of the formation. This increase in permeability will probably heal if, and when, the formation is allowed to return to a hydrostatic pressure state.

* One would speculate from the previous discussions of hydrostatic pressure measurements that it can be reversed by hydrostatic pressure and time, see also Table VII.

REFERENCES

1. W. R. Aufright and K. C. Howard, "Salt Characteristics As They Affect Storage of Hydrocarbons", J. Petroleum Tech., 13 (1961), p. 733.
2. S. Foerster, "Permeability and Fissuring Studies to Ascertain the Imperviousness of Salt Caverns", Neue Bergbautechnik, 4 (1974), p. 278, (J. W. Crabbs, Translator, ORNL-TR-4507).
3. E. Hofrichter "Porosity and Permeability of Saliferous Rocks", Erdoel-Erdgas-Zeitschrift, 92 (1976) p. 77, (J. W. Crabbs, Translator, ORNL-TR-4506).
4. "Special Core Analysis Study for Sipes, Williamson and Aycock, Inc.", Core Labs, Inc., Dallas, TX, March 1977.
5. C. H. Cooley, S. W. Butters, and A. H. Jones, "Permeability of Rock Salt to Gases and Liquids", TR 78-62, Terra Tek, Salt Lake City, November 1978, 19 p.
6. J. E. Shelby, "Permeability of Sodium Chloride", Sandia Laboratories Internal Memorandum, February 1978.
7. W. F. Brace, J. B. Walsh, and W. T. Frangos, "Permeability of Granite Under High Pressure", J. Geophysical Res., 73 (1968), p. 2225.
8. Recommended Practice for Determining Permeability of Porous Media, API RP27, 3rd Ed., Aug., 1956, 27 p.
9. A. C. Jenkins and G. A. Cook, "Gas Phase Properties", Chap. VII of Argon, Helium, and The Rare Gases, (G. A. Cook, ed.) Interscience, 1961.
10. W. R. Wawersik, "Large Specimen Triaxial Apparatus for Rock Testing to 70 MPa Confining Pressure and 225°C", (in publication).
11. W. R. Wawersik and D. W. Hannum, "Mechanical Behavior of New Mexico Rock Salt in Triaxial Compression Up to 200°C", J. Geophysical Res., (in press).
12. M. Muskat and R. D. Wyckoff, The Flow of Homogeneous Fluids Through Porous Media, McGraw-Hill, 1937.
13. L. J. Klinkenberg, "The Permeability of Porous Media to Liquids and Gases", Drilling and Production Practice, 2 (1941), p. 200.

TABLE I

Hydrostatic Pressure

Summary of Results
Spec. No. 9-2103

Test No.	Gas Pressure		Confining Pressure		Permeability ud	Comments
	MPa	(psi)	MPa	(psi)		
1A	9.1	(1314)	13.8	(2008)	8.51	'Raw' Core
2A	9.0	(1305)	13.8	(2002)	8.50	Repeat
3A	9.0	(1303)	13.8	(1997)	8.44	Repeat
4A	8.9	(1286)	13.8	(1957)	8.62	Repeat
5A	8.8	(1281)	20.6	(2991)	6.86	
6A	8.8	(1278)	20.4	(2960)	6.72	Repeat
7A	8.8	(1278)	27.9	(4050)	2.46	
8A	8.8	(1275)	27.6	(4001)	2.27	Repeat
9A	8.8	(1270)	34.4	(4995)	0.81	
10A	8.8	(1270)	33.9	(4915)	0.69	Repeat
11A	8.7	(1265)	27.8	(4032)	0.67	
12A	8.7	(1260)	21.1	(3062)	0.72	
13A	8.7	(1256)	14.1	(2048)	0.91	
14A	8.7	(1255)	14.5	(2098)	0.91	
15A	8.3	(1210)	14.5	(2102)	0.97	Repeat, Reverse Flow
16A	9.0	(1298)	14.3	(2068)	1.01	Overnight Without Confining Pressure
17A	8.9	(1295)	20.8	(3019)	0.74	
18A	8.9	(1292)	28.0	(4059)	0.63	
19A	8.9	(1288)	35.2	(5097)	0.42	
20A	8.7	(1265)	34.4	(4995)	0.24	2 Hr. Hold Period
21A	8.7	(1262)	27.8	(4025)	0.23	
22A	8.7	(1258)	21.1	(3061)	0.26	
23A	8.7	(1255)	13.9	(2010)	0.37	
24A	8.2	(1185)	14.2	(2066)	0.34	Overnight With Confining Pressure
1B	9.3	(1350)	14.0	(2033)	0.77	Several Months Later After Rough Machining And Then Remachined
2B	9.3	(1345)	13.9	(2010)	0.81	
3B	9.2	(1340)	13.8	(2002)	0.85	Repeat
4B	9.2	(1338)	20.7	(3005)	0.61	
5B	9.2	(1335)	20.7	(3005)	0.60	Repeat
6B	9.2	(1330)	20.7	(3006)	0.58	Repeat
7B	9.1	(1326)	14.0	(2025)	0.68	
8B	9.1	(1326)	14.0	(2025)	0.73	Repeat
9B	9.1	(1322)	10.4	(1511)	1.48	

TABLE II
Hydrostatic Pressure

Summary of Results
Spec. No. 9-21C5

Test No.	Gas Pressure		Confining Pressure		Time hrs.	Permeability μ d	Comments
	MPa	(psi)	MPa	(psi)			
1A	10.9	(1581)	14.3	(2067)	0.5	3.28	'Raw' Core
2A	10.8	(1573)	14.0	(2034)	0.8	3.25	
3A	10.8	(1569)	14.0	(2023)	1.2	3.26	
4A	10.8	(1566)	13.9	(2014)	1.4	3.25	
5A	10.8	(1560)	13.8	(1996)	2.1	3.33	
6A	10.7	(1551)	13.6	(1978)	3.0	3.38	
7A	10.7	(1548)	14.0	(2025)	3.6	3.23	
8A	10.6	(1534)	13.9	(2010)	4.1	3.23	
9A	10.6	(1530)	13.8	(2008)	4.5	3.20	
10A	10.5	(1525)	13.8	(2001)	5.0	3.19	
11A	10.5	(1516)	13.8	(2008)	6.3	3.11	
12A	10.0	(1454)	14.0	(2025)	23.5	2.66	Av of 3
13A	9.9	(1434)	13.9	(2021)	30.6	2.56	Av of 2
14A	10.2	(1475)	14.0	(2036)	47.5	2.36	Av of 2
15A	9.6	(1385)	13.7	(1990)	54	2.11	Av of 2
16A	10.8	(1569)	14.0	(2033)	72	2.01	Av of 2
17A	10.6	(1533)	13.9	(2021)	81	1.92	Av of 2
18A	9.2	(1336)	14.2	(2065)	143	1.12	Av of 2
19A	9.0	(1306)	13.7	(1990)	151	1.21	Av of 2
20A	8.9	(1285)	14.1	(2051)	167	1.16	Av of 2
21A	10.2	(1480)	13.9	(2019)	191	1.24	Av of 2
22A	10.2	(1475)	20.9	(3030)	192	0.57	Av of 2
23A	10.1	(1469)	28.0	(4060)	192	0.15	Av of 2
24A	10.1	(1462)	34.2	(4963)	193	<0.05	
25A	10.0	(1448)	27.8	(4031)	194	<0.05	
26A	9.9	(1440)	20.5	(2973)	195	<0.05	
27A	9.8	(1425)	14.2	(2058)	198	<0.05	
28A	9.7	(1404)	13.8	(2006)	215	<0.05	
1B	10.7	(1556)	13.8	(2003)	2.5	1.83	Several Months After Machining Av of 3
2B	10.7	(1555)	20.6	(2989)	4.0	1.18	Av of 3
3B	10.6	(1532)	28.0	(4056)	4.5	0.53	
4B	10.5	(1525)	27.8	(4025)	5.2	0.47	Av of 2
5B	10.5	(1522)	34.8	(5051)	5.7	0.20	
6B	10.5	(1516)	34.4	(4985)	6.3	0.10	
7B	10.4	(1513)	34.3	(4975)	6.8	0.07	
8B	10.4	(1509)	27.8	(4027)	7.0	0.07	
9B	10.4	(1509)	21.1	(3055)	7.3	0.09	
10B	10.4	(1509)	14.0	(2023)	7.6	1.64	
11B	10.2	(1478)	14.0	(2028)	24.2	1.47	Overnight Av of 2

TABLE II

Hydrostatic Pressure

Test No.	Gas Pressure		Confining Pressure		Time hrs.	Permeability μ d	Comments
	MPa	(psi)	MPa	(psi)			
12B	10.1	(1466)	20.8	(3010)	25.7	0.08	Av of 2
13B	10.0	(1456)	27.8	(4029)	26.6	<0.05	Av of 2
14B	9.9	(1438)	34.6	(5021)	28.4	<0.05	Av of 2
15B	9.8	(1428)	27.8	(4025)	29.2	<0.05	
16B	9.8	(1424)	20.9	(3025)	29.8	<0.05	
17B	9.8	(1418)	14.4	(2086)	30.4	<0.05	
18B	9.6	(1398)	13.8	(1997)	47.8	<0.05	Overnight
19B	9.6	(1385)	10.4	(1505)	49.2	0.20	Av of 2
20B	6.2	(892)	7.0	(1011)	50.3	0.19	Av of 3
21B	2.7	(393)	3.6	(529)	56.6	0.12	Av of 2

TABLE III
Hydrostatic Pressure

Summary of Results
Spec. No. 9-2601.5

Test No.	Gas Pressure		Confining Pressure		Time hrs.	Permeability μ d	Comments
	MPa	(psi)	MPa	(psi)			
1B	7.9	(1151)	13.8	(2002)	1.4	3.64	Subjected To Prior Strain History

TABLE IV
Hydrostatic Pressure

Summary of Results
Spec. No. 9-2609

Test No.	Gas Pressure		Confining Pressure		Permeability μd	Comments
	MPa	(psi)	MPa	(psi)		
1A	3.7	(540)	6.6	(961)	0.64	
2A	9.9	(1430)	13.2	(1918)	0.45	'Raw' Core
3A	9.8	(1425)	20.5	(2968)	0.29	Raise Gas Pressure
4A	9.6	(1419)	13.8	(2006)	0.32	
5A	10.0	(1455)	14.0	(2036)	0.15	Overnight
6A	10.0	(1446)	20.4	(2962)	0.12	
7A	9.9	(1430)	27.8	(4033)	0.06	
8A	9.8	(1423)	34.5	(5005)	0.08	
9A	9.8	(1414)	27.8	(4035)	0.05	
10A	9.7	(1408)	14.7	(2134)	0.18	
11A	9.8	(1428)	14.0	(2025)	0.10	Overnight
12A	10.7	(1550)	14.0	(2030)	0.10	Repeat
13A	10.6	(1534)	14.0	(2023)	<0.05	5 Days
14A	10.5	(1521)	21.1	(3054)	<0.05	
15A	10.4	(1515)	14.2	(2062)	0.06	
16A	7.0	(1010)	14.1	(2045)	0.06	Lower Gas Pressure
17A	3.5	(505)	13.9	(2010)	0.07	Lower Gas Pressure

TABLE V
Hydrostatic Pressure

Summary of Results
Spec. No. 9-2610

Test No.	Gas Pressure		Confining Pressure		Time hrs.	Permeability μ d	Comments
	MPa	(psi)	MPa	(psi)			
1A	10.7	(1548)	14.0	(2025)	0.83	<0.05	'Raw' Core
2A	10.5	(1526)	13.9	(2010)	0.87	<0.05	
3A	10.5	(1526)	13.8	(2003)	1.5	<0.05	
4A	10.3	(1494)	13.5	(1963)	5.5	0.05	Reverse Flow
5A	10.2	(1484)	13.5	(1960)	5.5	0.06	
1B	7.9	(1150)	13.9	(2020)	---	<0.05	Several Months After Machining Start Of Differential Pressure Measurements

TABLE VI

Hydrostatic Pressure

Summary of Results
Spec. No. 9-2613

Test No.	Gas Pressure		Confining Pressure		Time hrs.	Permeability μ d	Comments
	MPa	(psi)	MPa	(psi)			
1A	9.3	(1346)	13.1	(1905)	---	0.61	'Raw' Core
2A	9.3	(1342)	13.1	(1900)	---	0.51	Repeat
3A	8.7	(1265)	13.0	(1888)	---	0.62	Reverse Flow
1B	8.7	(1255)	14.3	(2077)	1.5	4.51	Several Months After Machining
2B	8.7	(1255)	14.3	(2080)	1.9	4.57	
3B	8.7	(1255)	14.3	(2079)	2.2	4.61	
4B	8.6	(1249)	14.3	(2077)	2.8	4.53	
5B	8.6	(1245)	14.3	(2074)	3.7	4.51	
6B	8.6	(1241)	14.3	(2070)	4.3	4.43	
7B	8.6	(1241)	14.2	(2066)	4.8	4.39	
8B	8.5	(1236)	14.2	(2059)	5.6	4.23	
9B	8.5	(1234)	14.1	(2049)	5.8	4.11	
10B	8.5	(1231)	14.3	(2074)	7.5	3.96	
11B	8.5	(1231)	14.1	(2039)	14.4	3.41	Av of 2
12B	10.2	(1484)	14.2	(2062)	23.8	3.53	Av of 2, Paise Pore Pressed
13B	10.2	(1474)	14.2	(2054)	28.0	3.38	Av of 2
14B	10.1	(1466)	13.9	(2012)	31.4	3.40	Av of 2
15B	10.1	(1468)	14.2	(2055)	47.6	2.81	Av of 2
16B	10.0	(1445)	14.0	(2026)	54.7	2.66	Av of 2
17B	9.9	(1435)	14.1	(2043)	71.5	2.14	Av of 2
18B	9.8	(1428)	14.1	(2043)	77.6	1.91	Av of 2
19B	9.7	(1411)	14.0	(2030)	95.3	1.60	Av of 2
20B	9.6	(1397)	14.0	(2028)	103	1.45	Av of 2
21B	9.4	(1359)	14.0	(2033)	168	0.78	Av of 2
22B	9.3	(1342)	14.0	(2030)	175	0.79	Av of 2
23B	9.2	(1330)	13.8	(2008)	191	0.64	Av of 2
24B	9.1	(1316)	13.9	(2010)	199	0.55	Av of 2
25B	10.2	(1480)	14.1	(2050)	215	0.42	Av of 4
26B	9.0	(1310)	14.1	(2044)	263	0.21	Av of 2
27B	8.3	(1205)	14.1	(2043)	336	0.20	Av of 4
1C	9.9	(1435)	21.1	(3060)	340	<0.05	Start Of Dif- ferential Pressure Test

TABLE VII
Hydrostatic Pressure

Summary of Results
Spec. No. 9-2671.5

Test No.	Gas Pressure		Confining Pressure		Time hrs.	Permeability μ d	Comments
	MPa	(psi)	MPa	(psi)			
1B	7.9	(1140)	14.1	(2051)	2.8	1000.	Subjected To Prior Strain History
2B	7.9	(1145)	20.8	(3020)	3.8	710.	2 Days Later
3B	7.9	(1151)	20.9	(3027)	73.0	410.	

TABLE VIII

Differential Pressure

Summary of Results
Spec. No. 9-2610

Test No.	Gas Pressure		Confining Pressure		Diff Pressure		Time hrs.	Perm μ d	Comments
	MPa	(psi)	MPa	(psi)	MPa	(psi)			
1C	7.9	(1150)	13.9	(2020)	0	(0)	0	0.05	"Healed"
2C	7.9	(1148)	13.9	(2019)	6.9	(1000)	0.17	0.05	
3C	7.9	(1141)	13.8	(2003)	13.8	(2000)	0.88	0.05	
4C	7.9	(1149)	15.1	(2192)	20.7	(3000)	1.42	0.05	
5C	7.9	(1146)	13.6	(1977)	27.6	(4000)	1.97	0.05	
6C	7.9	(1142)	13.8	(2000)	34.5	(5000)	2.50	0.2*	
7C	7.9	(1148)	13.8	(1998)	41.4	(6000)	3.00	0.5*	
8C	7.9	(1145)	13.7	(1990)	48.3	(7000)	3.50	0.5*	
9C	7.9	(1141)	13.7	(1987)	55.2	(8000)	4.17	0.3*	
10C	7.8	(1138)	13.6	(1979)	0	(0)	4.38	0.1	

* Apparent permeability measured with a changing capacity.

TABLE IX

Differential Pressure

Summary of Results
Spec. No. 9-2613

Test No.	Gas Pressure		Confining Pressure		Diff Pressure		Time hrs.	Perm Md	Comments
	MPa	(psi)	MPa	(psi)	MPa	(psi)			
1C	9.9	(1435)	21.1	(3060)	3.4	(500)	0.25	<0.05	"Healed" To Full Compaction
2C	9.9	(1435)	21.1	(3056)	6.9	(1000)	0.53	<0.05	
3C	9.9	(1429)	21.1	(3055)	10.3	(1500)	0.80	<0.05	Diff Pressure Reduced
4C	9.7	(1410)	21.0	(3049)	0.9	(125)	3.50	<0.05	
5C	9.7	(1408)	21.0	(3042)	10.3	(1500)	3.77	<0.05	
6C	9.7	(1405)	20.9	(3037)	13.8	(2000)	4.04	<0.05	
7C	9.7	(1400)	20.9	(3031)	17.2	(2500)	4.30	<0.05	
8C	9.6	(1394)	20.8	(3020)	20.7	(3000)	4.57*	<0.05	
9C	9.6	(1390)	20.8	(3021)	24.1	(3500)	4.84*	<0.05	
10C	9.6	(1385)	20.8	(3012)	27.5	(4000)	5.10*	<0.05	
11C	9.6	(1383)	20.7	(3007)	31.0	(4500)	5.37*	<0.05	
12C	9.5	(1380)	20.8	(3009)	34.5	(5000)	5.64*	0.06	
13C	9.5	(1378)	20.8	(3009)	37.9	(5500)	5.90*	0.08	
14C	9.5	(1376)	20.7	(3006)	41.4	(6000)	6.17*	0.08	
15C	9.5	(1374)	20.6	(2993)	0.9	(125)	6.44	<0.05	Held Overnight At Confining Pressure
16C	9.2	(1330)	20.7	(3002)	0.9	(125)	23.00	<0.05	
17C	9.2	(1328)	21.0	(3044)	34.5	(5000)	24.25	<0.05	
18C	9.1	(1326)	21.0	(3048)	37.9	(5500)	24.52	<0.05	
19C	9.1	(1324)	21.0	(3042)	41.4	(6000)	24.78*	<0.05	
20C	9.1	(1322)	21.0	(3042)	44.9	(6500)	25.05*	0.06	
21C	9.1	(1320)	20.9	(3037)	48.3	(7000)	25.32*	0.07	
22C	9.0	(1311)	20.9	(3033)	51.7	(7500)	25.58*	0.08	
23C	9.0	(1307)	20.9	(3028)	55.2	(8000)	25.85*	0.09	
24C	9.0	(1305)	20.9	(3028)	58.6	(8500)	26.12*	0.10	
25C	9.0	(1302)	20.8	(3022)	62.1	(9000)	26.38*	0.11	
26C	9.0	(1299)	20.9	(3020)	65.5	(9500)	26.65*	0.13	
27C	9.0	(1298)	20.9	(3018)	69.0	(10000)	26.92*	0.14	
28C	8.9	(1288)	20.9	(3018)	0.3	(50)	27.18	<0.05	
29C	10.5	(1517)	20.8	(3011)	0.3	(50)	171.75	<0.05	Without Confining Pressure

* Apparent permeability measured with a changing capacity.

FIGURE 1

Test Data from Test 11B-1, 9-2613

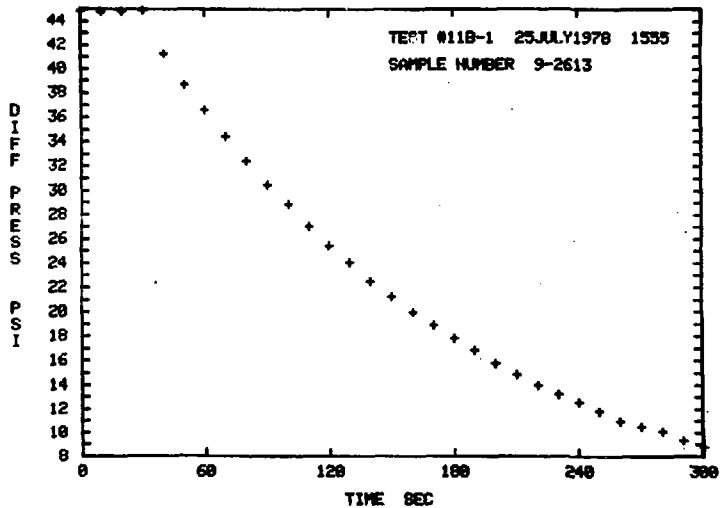


FIGURE 2

Logarithmic Data from Test 11B-1, 9-2613

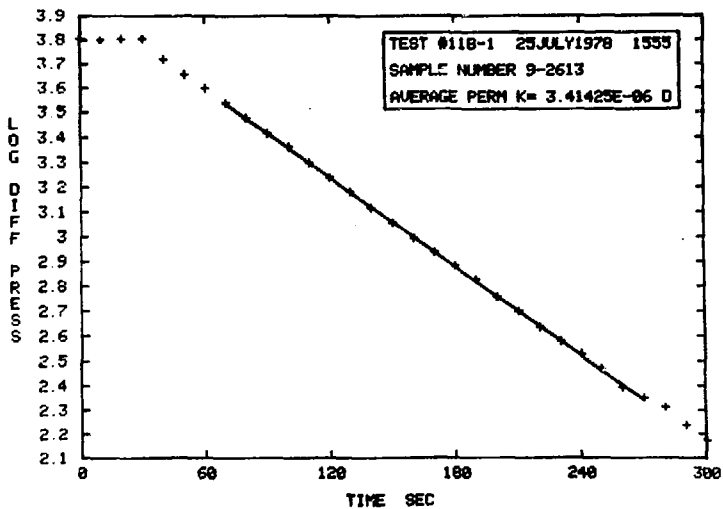


FIGURE 3
Experimental Setup

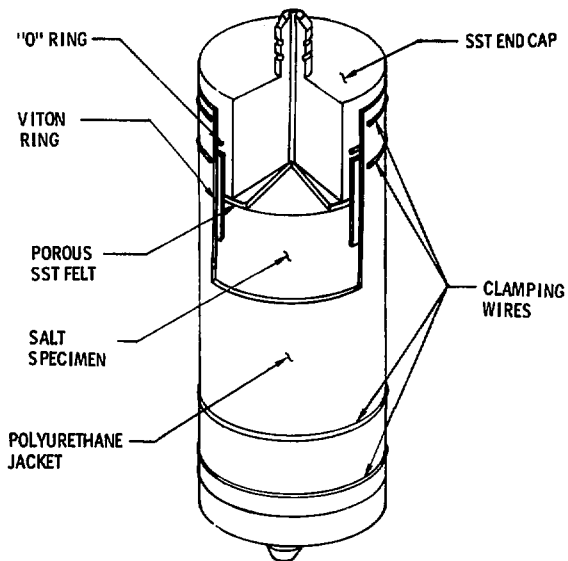


FIGURE 4

Test Series A for 9-2103

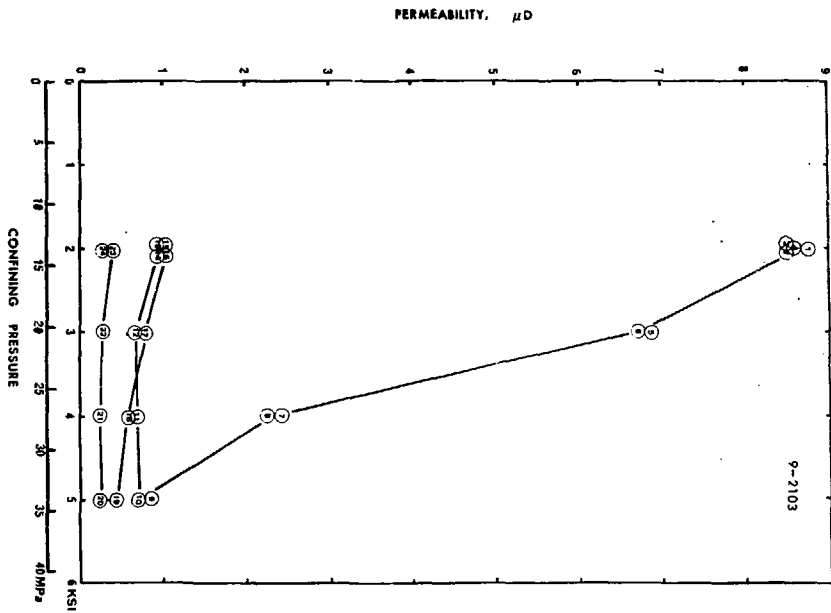


FIGURE 5
Test Series A for 9-2609

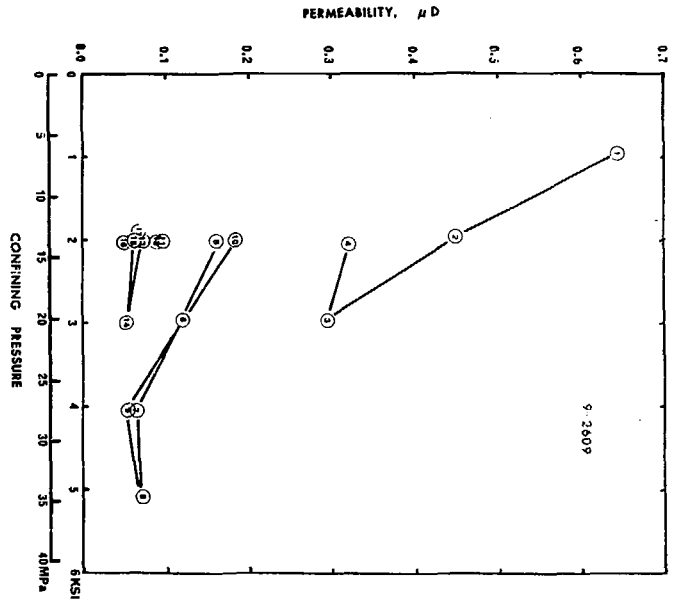


FIGURE 6
Test Series A for 9-2105

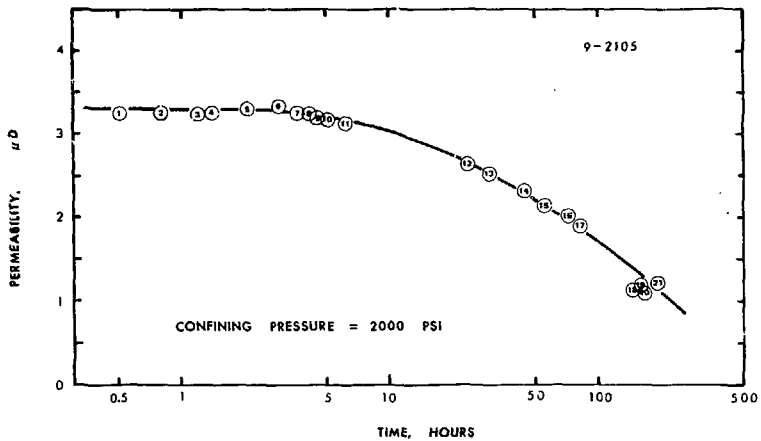


FIGURE 7

Test Series B for 9-2613

